

LIBRARY
ROYAL AIRCRAFT ESTABLISHMENT
BEDFORD.



MINISTRY OF AVIATION
AERONAUTICAL RESEARCH COUNCIL
CURRENT PAPERS

Free-Flight Measurements of the Zero-Lift Drag
of a Slender Ogee Wing at Transonic and
Supersonic Speeds.

By

J.B.W. Edwards

LONDON: HER MAJESTY'S STATIONERY OFFICE

1964

Price 3s 6d net

FREE-FLIGHT MEASUREMENTS OF THE ZERO-LIFT DRAG OF A SLENDER OGEE WING
AT TRANSONIC AND SUPERSONIC SPEEDS

by

J. B. W. Edwards

SUMMARY

The zero-lift drag of a slender-wing model has been measured using the free-flight technique and the wing wave drag has been deducted by subtracting the non-wave-drag components.

The results are presented without correction for the drag increment caused by the transition strip and show a smooth variation of the wave drag factor K_D with Mach number with a maximum occurring near $M = 1.1$. The overall level of K_D is some 10% higher than that predicted by linear theory, but this result is very dependent on the accuracy of the skin-friction estimates as well as on the transition strip drag increment. Attempts to estimate the latter suggest that 4% of the total drag may arise from this source which would reduce K_D by some 12% bringing it well in line with theory.

LIST OF CONTENTS

	<u>Page</u>
1. INTRODUCTION	3
2. WING SHAPE	3
3. DESCRIPTION OF MODEL AND TEST TECHNIQUE	4
3.1 Model design	4
3.2 Test technique	4
4. RESULTS AND DISCUSSION	5
4.1 Total drag measurements	5
4.2 Fin and sting drag	5
4.3 Wing friction drag	5
4.4 Wing wave drag	6
4.5 Discussion	6
5. CONCLUSIONS	7
LIST OF SYMBOLS	8
LIST OF REFERENCES	8
ILLUSTRATIONS - Figs. 1-6	-
DETACHABLE ABSTRACT CARDS	-

LIST OF ILLUSTRATIONS

	<u>Fig.</u>
General arrangement of the model	1
Spanwise variations of wing thickness	2
Cross-section area distribution	3
Photograph of the free-flight model	4
Variation of drag with Mach number	5
Zero-lift wing wave drag factor K_0	6

1. INTRODUCTION

A considerable amount of theoretical and experimental work has been done on the slender wing to investigate its suitability for a supersonic transport aircraft. Many lessons have been learnt from this work and a number of shapes, representing plausible layouts bearing in mind results obtained on cruising efficiency and on low-speed behaviour, have been proposed for more detailed investigations. The brunt of the work on these shapes falls on wind-tunnel experiments, but free-flight tests on one of the shapes have been made. Tunnel tests have confirmed the general trends in supersonic drag indicated by theory; free-flight tests were made to check on this, and, more important, to provide information at transonic speeds because this is a critical region for such an aircraft, there is no adequate theory and tunnel tests are of doubtful reliability.

This note describes measurements of the zero-lift drag at transonic speeds and at supersonic speeds up to a Mach number of 2.6. Comparison with theory is made where such results are available.

2. WING SHAPE

The wing tested was uncambered and its planform is shown in Fig. 1.

The geometry of the planform is given by the equation

$$\frac{s}{c_0} = 0.2 \frac{x}{c_0} + 0.15 \left(\frac{x}{c_0}\right)^4 - 0.1 \left(\frac{x}{c_0}\right)^8$$

and hence

$$\frac{s_T}{c_0} = 0.25$$

where s = semi span at station x

s_T = semi span at the trailing edge

x = distance measured aft of the leading edge apex

c_0 = length of the centre line chord.

The planform shape parameter p which is the ratio of the area of the wing to that of its enclosing rectangle is 0.475.

The cross-section shapes at five chordwise stations are shown in Fig. 2 to illustrate the thickness distribution. Fig. 3 illustrates the longitudinal cross-section area distribution from which it can be seen that the distribution is smooth with its maximum at 61% of the root chord.

The size of the model was governed by the free-flight technique itself; the minimum was set by the volume required to house the telemetry and Doppler equipment and the maximum by the performance of available boost systems. This led to a model length of 80 inches with a maximum span at the trailing edge of 40 inches.

3. DESCRIPTION OF MODEL AND THE TEST TECHNIQUE

3.1 Model design

The model consisted of an aluminium-alloy plate 0.252 inches thick with its edges profiled to form the sharp leading and trailing edges of the wing. The rest of the wing was formed from two coatings of synthetic resin

(Araldite), forming skins on either side of the centre plate, which were shaped to the required contours and surface finish by wood-working methods. The nose was largely filled with a ballast weight to obtain a satisfactory centre-of-gravity position, and measuring instruments, telemetry set and Doppler equipment were mounted on the top side of the centre plate, access being provided by a removable cover in the upper skin. This cover can be seen in the photograph of model shown in Fig. 4a. An opening was provided in the lower skin to accommodate the boost-motor hook which transmits the loads between model and boost during the acceleration period of the flight. When the model leaves the hook on separation a spring-loaded door closes the aperture and restores the wing surface to its correct profile.

The stabilizing fin was formed from an aluminium-alloy plate and was of straight-tapered planform with a streamwise tip, and leading-edge sweepback of 55° : the section shape was a modified double wedge with a constant thickness : chord ratio of 0.03 (Fig. 1). In order to try and minimise aerodynamic-interference effects between the fin and wing, the fin was mounted on a cylindrical sting extending 13 inches aft of the wing trailing edge (Fig. 1). The presence of the sting obviously effects the wing profile near the trailing edge, but any effect on the total drag should be small since the effect of the sting on the centre-line area distribution was small as can be seen in Fig. 3. Measurements of this effect on a similar model in tunnel tests suggest that the presence of the sting causes a reduction in drag due to increased pressures near the trailing edge of 0.00025 in C_D , that is a reduction of about 3% in total drag.

The sting was also fitted with a pyrotechnic flare, which burned throughout the flight as an aid to visual tracking, and a pressure tapping in the base so that in-flight measurements of base pressure and hence base drag could be obtained. The sting base drag was very small indeed in practice.

The model was fitted with instruments to measure longitudinal accelerations, normal accelerations at the C.G. and at a point well aft of the C.G., lateral acceleration at the C.G. and the sting base pressure; a signal was also transmitted to indicate that the door covering the hook aperture had closed satisfactorily. Readings from the instruments were telemetered to ground by means of a standard 455 m/cs telemetry set. The model also carried a Doppler transponder used for the accurate determination of velocity and trajectory. The aeriials for both Doppler and telemetry transmissions were arranged to cause no aerodynamic interference, the former being a pair of slots cut in the wing trailing edge and the latter a single slot cut in the fin trailing edge. The slots were filled with resin to leave a smooth external profile.

3.2 Test technique

The model was carried pick-a-back on a single solid-fuel rocket motor, held in position by the hook mounted on the motor engaging into the opening in the under surface of the model. The sting end was also located in a socket on the boost to prevent any pitching or yawing of the model and outriggers on the boost restrained the model from rolling relative to the rocket motor.

The first model to be flown was boosted to its maximum Mach number of about 1.6 and the second which was a more powerful rocket motor reached a maximum Mach number of 2.6. When the boost motor finished burning the model moved forward relative to the boost and disengaged itself from the hook since the drag/weight ratio of the model is lower than that of the boost system. The model then continued in a zero-lift trajectory slowing down under the influence of aerodynamic drag; all the measurements relevant to the experiment were taken during this period of coasting flight. The trajectory and velocity were obtained from kine-theodolites and multi-station Doppler.

4 RESULTS AND DISCUSSION

Two models were flown, the first was successful and has provided results from a Mach number of 1.6 through the transonic speed range down to $M = 0.98$. The second was intended to cover a higher speed range from $M = 2.6$ down to 1.2 to link up with the results from the first one. The telemetry transmission on this second model ceased shortly before separation from the boost and thus the readings of all instruments were lost. Since it is possible to derive reasonable drag data from sources other than the longitudinal accelerometers this in itself was not too serious a loss but unfortunately the kine-theodolite and Doppler information was also very poor. Consequently, results are only available for the very early part of the trajectory and since the drag even for this part has to be obtained by differentiating the velocity record, it was thought that only a spot point at $M = 2.5$ could be presented with confidence.

4.1 Total drag measurements

The drag of the first model was deduced from the longitudinal accelerometers and by differentiating the velocity-time data from Doppler measurements. The general level of the drag was best deduced from the velocity data and the detailed shape of the curve, especially around sonic speed, was obtained from the accelerometer records since the smoothing process necessary to obtain drag from velocity data inevitably covers up any detail in the shape of the curve. Model 1 in fact reached a speed as low as $M = 0.9$ but the deceleration was then so small that it is not possible to measure it with sufficient accuracy and results have been obtained only down to $M = 0.98$. As mentioned above, model 2 gave results between $M = 2.4$ and 2.6 only and after smoothing the velocity data to obtain drag it was only justifiable to present a single reading at $M = 2.5$.

The measured total drag from both models is shown in Fig. 5.

4.2 Fin and sting drag

The fin wave drag was estimated using the linear-theory methods of Ref.3.

The fin skin-friction drag was estimated assuming that transition occurred at the leading edge and that conditions of full heat transfer obtained. The second assumption is based on the fact that the flight was of very short duration and that the fin was made from aluminium alloy which has a reasonably high heat capacity and is also a good heat conductor.

Similar assumptions were made to estimate the skin-friction drag of the sting, and the sting base drag was deduced from pressure measurements for model 1 and was estimated for model 2. These four contributions to the fin and sting drag have been added together and are shown plotted against Mach number in the drag breakdown in Fig.6. They contribute about 10% only to the total drag thus any errors in their estimation will have a negligible effect on the overall results.

4.3 Wing friction drag

Rather more than half the total drag was due to skin friction on the wing. This implies that the accuracy to which the wave drag of the wing can be extracted from the total drag is to large extent dependent of the accuracy of the skin-friction estimates.

The wing was fitted with a roughness strip in order to fix transition at the leading edge. This roughness consisted of particles of 90 grade (0.007 inch) Carborundum grit mixed in aluminium paint. It was applied in a band, half an inch wide, and $1/10$ " in from the leading edge, along the whole length, on both upper and lower surfaces of the leading edge. The Reynolds number, based on the geometric chord, \bar{c} ($= 3.16$ ft.) varies from 15×10^6 to 34×10^6 for model 1 and was 51×10^6 for model 2.

The high Reynolds numbers and the presence of roughness together should ensure that the flow over the whole of the wing was fully turbulent. The roughness band was set in from the leading edge so that no particles of grit would affect the sharp profile of the edge..

The friction estimates were made using the intermediate-enthalpy theory for flat-plate conditions. A correction was made to allow for the additional wetted area due to wing thickness. The degree of heat transfer assumed can radically affect the skin-friction estimates and as the conditions are transient during a free-flight test, estimates of the heat transfer had to be made.

These estimates were based on a step-by-step integration of the aerodynamic heat inputs using the known trajectory data and taking into account the heat capacity and thermal conductivity of the wing material.

The skin friction was then calculated assuming these "most-probable" heat-transfer conditions applied and is shown in Fig. 5. In order to illustrate the significance of the heat-transfer conditions on the skin friction, estimates assuming full and zero heat-transfer have been made and are also shown in Fig. 5. Since the skin of the wing was made from synthetic resin which is a good heat insulator, the wing surface temperatures follow fairly closely the recovery temperature and the estimates based on the most probable heat-transfer conditions lie much closer to the zero-heat-transfer than to full heat-transfer conditions. It should be made clear that the two additional estimates are not intended to indicate the limits of accuracy of the skin friction estimate. The "most probable" conditions are expected to be within $\pm 10\%$ of the true value of heat-transfer conditions.

No attempt has been made to allow for the affects of pressure gradients on skin friction nor have three-dimensional effects been considered.

4.4 Wing wave drag

The wave drag was taken to be the difference between the measured total drag and the sum of the wing friction, fin and sting drags. The wave drag is presented as a wave drag coefficient K_0 which is defined as

$$K_0 = C_{D_W} \frac{\pi}{128} \frac{S \ell^4}{V^2}$$

where C_{D_W} = wave drag coefficient

S = wing area, sq. ft.

ℓ = wing overall length, ft

V = wing volume, cu. ft.

This has been calculated using the most-probable skin-friction estimate and is plotted in Fig. 6 together with theoretical estimates from both slender and linear theories. Also shown are measurements made in the 8' x 8' tunnel at R.A.E. Bedford, these results were from pressure measurements at a Reynolds number of 4.75×10^6 .

4.5 Discussion

The measured values of K_0 are roughly 10% higher than the theoretical values given by slender theory at Mach numbers above 1.1 and are some 20% above the values measured in the tunnel tests. It is believed that two factors may account for these discrepancies. Firstly, as has been mentioned previously the accuracy to which K_0 can be extracted is closely dependent on the correctness of the skin-friction estimates and some uncertainty no doubt arises from this cause either directly from the skin-friction estimates themselves or indirectly from the estimates of heat-transfer conditions.

Secondly, and probably of even greater significance are the errors caused by the presence of drag introduced by the transition band. Since the models were fired it has become clear that the roughness applied was too extensive and its grain size was much larger than necessary. A far from negligible contribution to the total drag has probably arisen from this source since its area was 5.4% of the total wing area. It is difficult to assess the drag increment that it would cause with accuracy but two estimates have been made. The first is based on Ref. 3, but the information presented there was based on subsonic measurements and was only intended to apply to roughness over all the wing surface. The second estimate was based on Ref. 4 in which the drag increment of roughness bands on delta wings was measured in supersonic wind-tunnel tests, but the bands were only $\frac{1}{4}$ " wide compared to $\frac{1}{2}$ " on the free-flight models and the roughness was not mixed in paint which will no doubt change the effective grain size in some way. However, both methods of estimation gave drag increments of the order of 4% of the total drag which if allowed for in the wave drag results would decrease the value of K_0 by about 12%. Such a change would bring the free-flight results almost in line with the theoretical values and in fair agreement with the tunnel tests. There is not sufficient evidence available on the drag increment caused by roughness bands to apply corrections to the results but it seems highly likely that this is a major contribution to the measured discrepancies.

The free-flight tests on a slender wing by Kell (Ref. 1), in which an identical roughness band was used, also showed a similar discrepancy between the measured and theoretical values of K_0 , hence the roughness band drag increment was probably the cause of the discrepancy in that experiment also.

The results at transonic speeds are of particular interest since it is most difficult to predict the trends theoretically. The supersonic theories predict that the value of K_0 will rise to infinity so the present results are important in that they show that no high peaks occur in the K_0 curve the maximum being about 24% above the cruise value. The value of K_0 reaches its maximum at $\frac{\beta s}{c} = 0.1$ which for this particular model corresponds to a Mach number just below 1.1.

5. CONCLUSIONS

The total zero-lift drag of a slender-wing model has been measured in free flight and the value of the wing wave drag has been deduced by subtracting the estimated non-wave components of the drag.

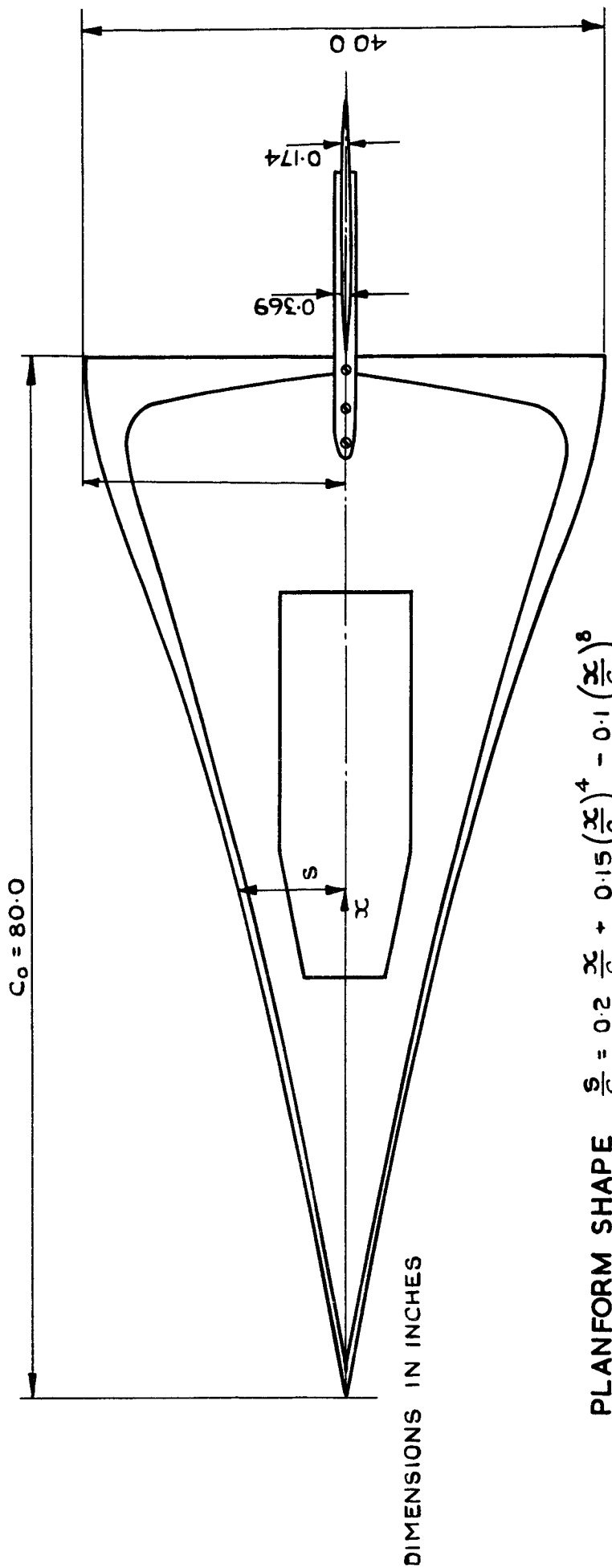
The results show a smooth variation of the wave drag coefficient K_0 at both transonic and supersonic speeds with a maximum of 1.17 occurring near a Mach number of 1.1. At supersonic speeds, the level of K_0 without correction for the transition strip drag is some 10% higher than that predicted by theory and almost 20% above values deduced from pressure measurements in tunnel tests. The accuracy of skin-friction estimates and the heat-transfer conditions have some effect on the accuracy with which K_0 can be extracted but the drag increment caused by the rather large transition band is most probably the major source of the discrepancies. There is insufficient evidence available to allow for this drag increment but estimates of it based on Refs. 3 and 4 suggest that it may be causing up to 4% of the total drag which in turn would reduce K_0 by about 12% bringing it more in line with both theoretical and tunnel-test values.

LIST OF SYMBOLS

c_o	centre-line chord length
C_{D_o}	zero-lift drag coefficient
C_{D_W}	wing wave-drag coefficient
K_o	$C_{D_W} \frac{\pi}{128} \frac{S c^4}{V^2}$
c	wing overall length
M	Mach number
p	ratio of wing planform area to area of enclosing rectangle $\left(= \frac{S}{2c_o s_T} \right)$
S	wing area
$S(x)$	cross-sectional area at station x
s	semi-span at station x
s_T	trailing-edge semi-span
V	wing volume
x	distance measured aft of wing apex
β	$\sqrt{M^2 - 1}$

LIST OF REFERENCES

<u>No.</u>	<u>Author</u>	<u>Title, etc.</u>
1	Kell, C.	Free-flight measurements of the zero-lift drag of a slender wing at Mach numbers between 1.4 and 2.7. R.A.E. Tech. Note No. Aero. 2779. Aug. 1961 A.R.C.23,511
2	Bishop, R.A. Cane, E.G.	Charts of the theoretical wave drag of wings at zero lift. A.R.C. Current Paper 313. June 1956
3	-	Royal Aeronautical Society Data Sheets. No. Wings 02.04.08
4	Firmin, M.C.P.	The drag of slender delta wings at supersonic speeds. R.A.E. Tech. Note No. Aero 2871. A.R.C.24,843.



PLANFORM SHAPE $\frac{s}{C_0} = 0.2 \frac{x}{C_0} + 0.15 \left(\frac{x}{C_0}\right)^4 - 0.1 \left(\frac{x}{C_0}\right)^8$

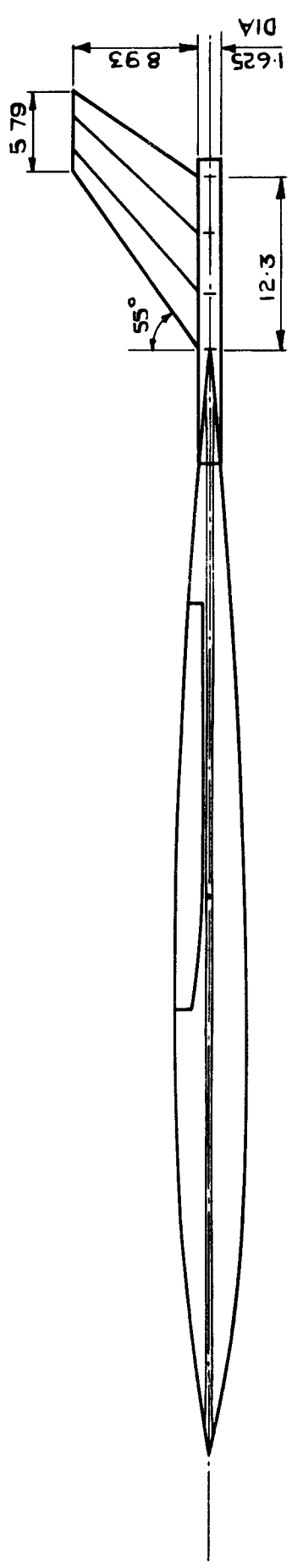


FIG. 1. GENERAL ARRANGEMENT OF THE MODEL.

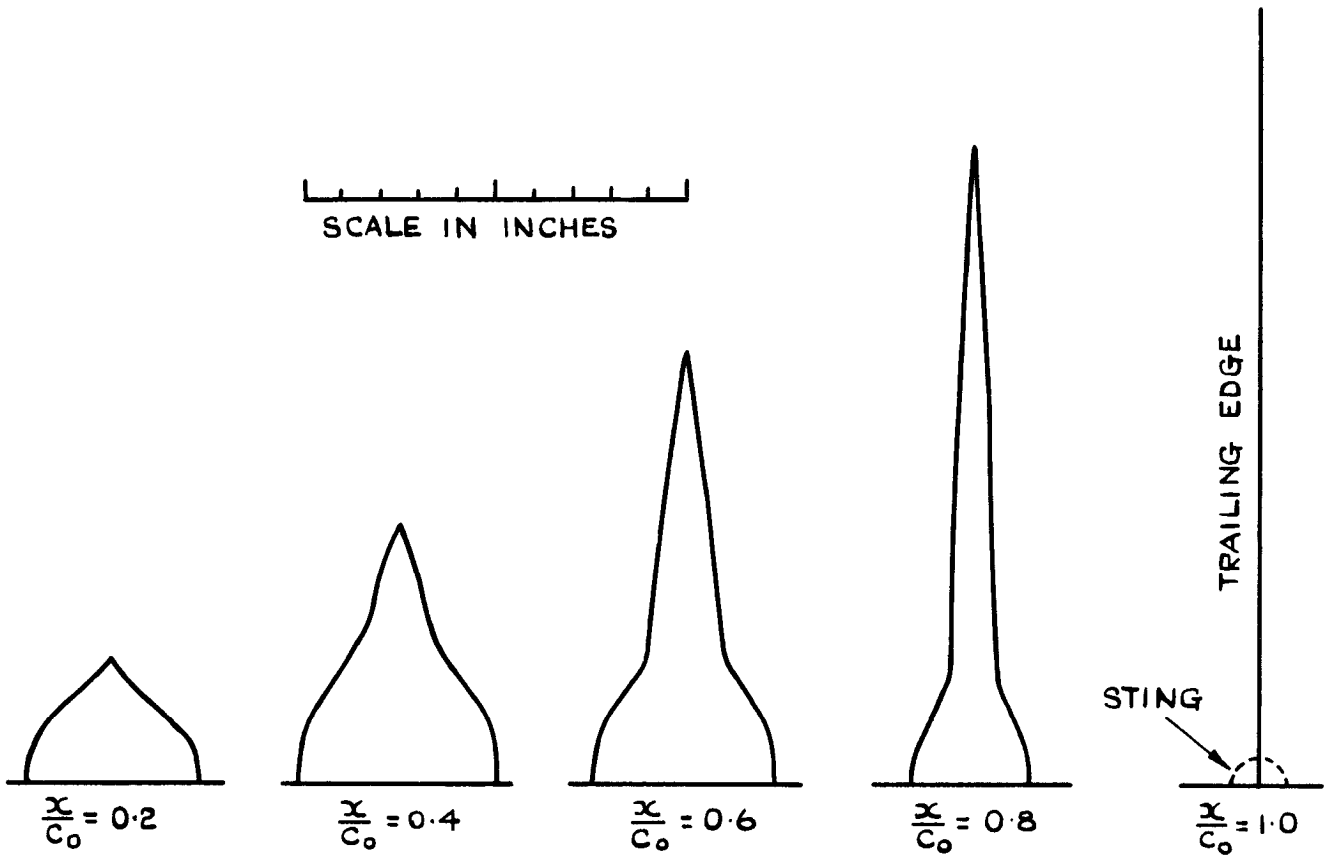


FIG.2. SPANWISE VARIATION OF WING THICKNESS.

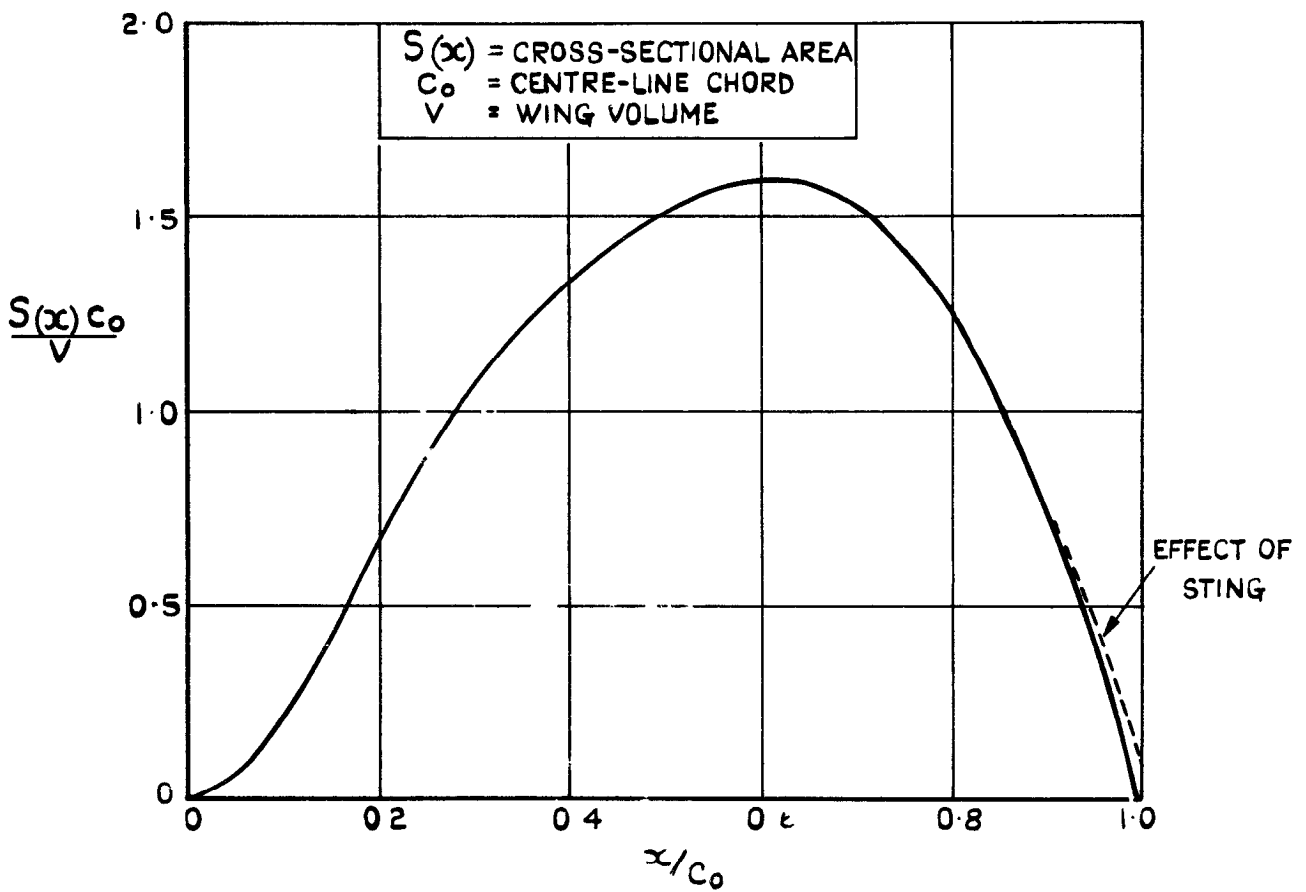


FIG.3. CROSS-SECTION AREA DISTRIBUTION.

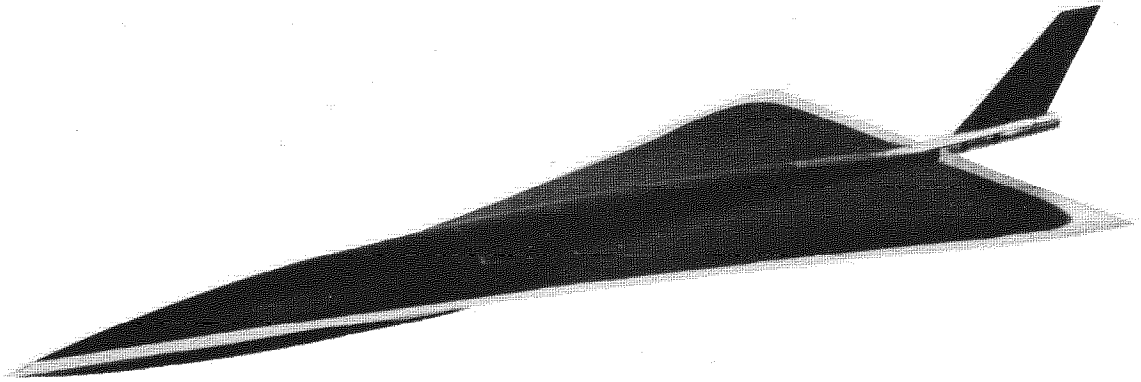


FIG.4 FREE FLIGHT MODEL

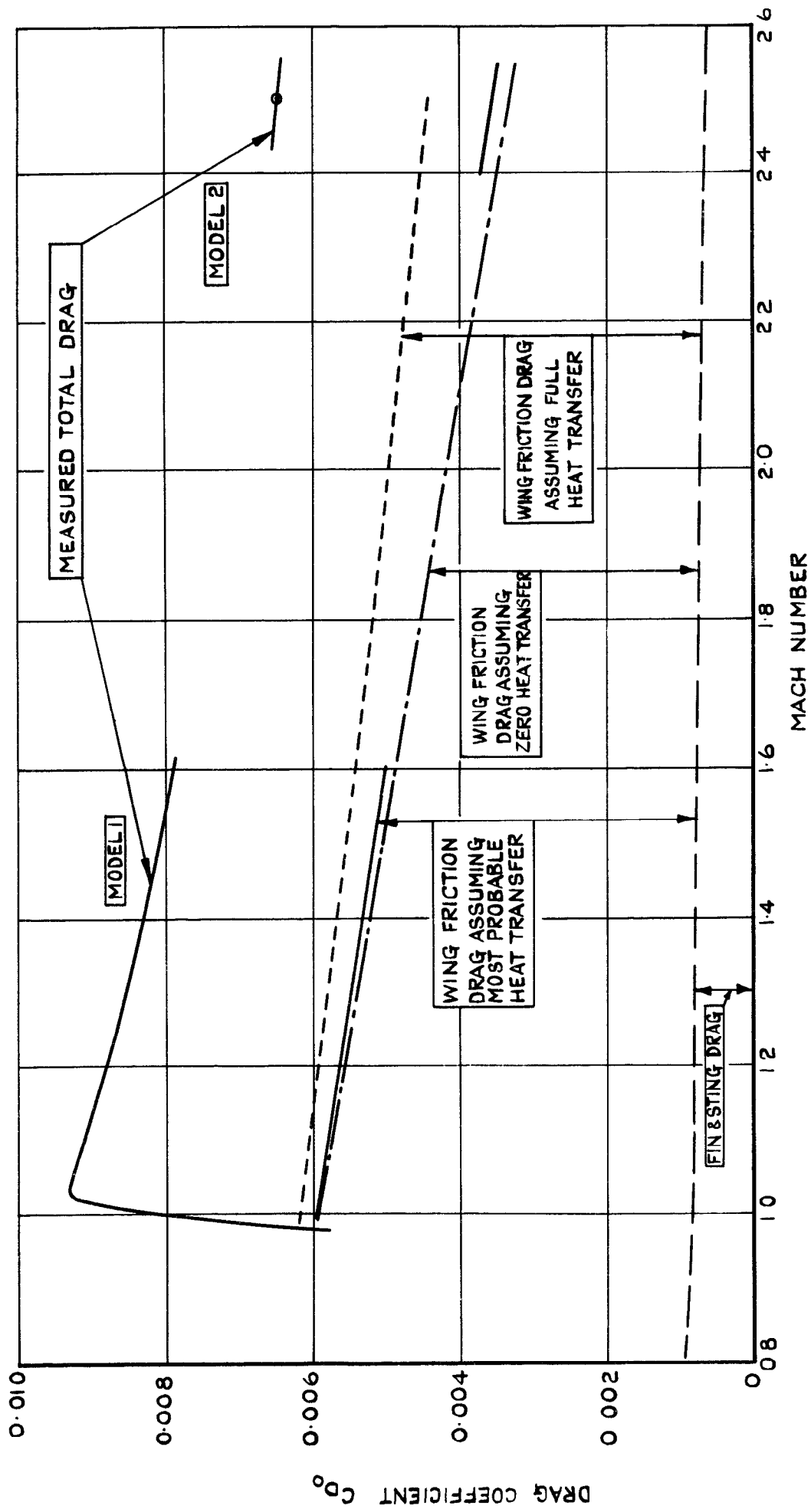


FIG. 5. VARIATION OF DRAG WITH MACH NUMBER.

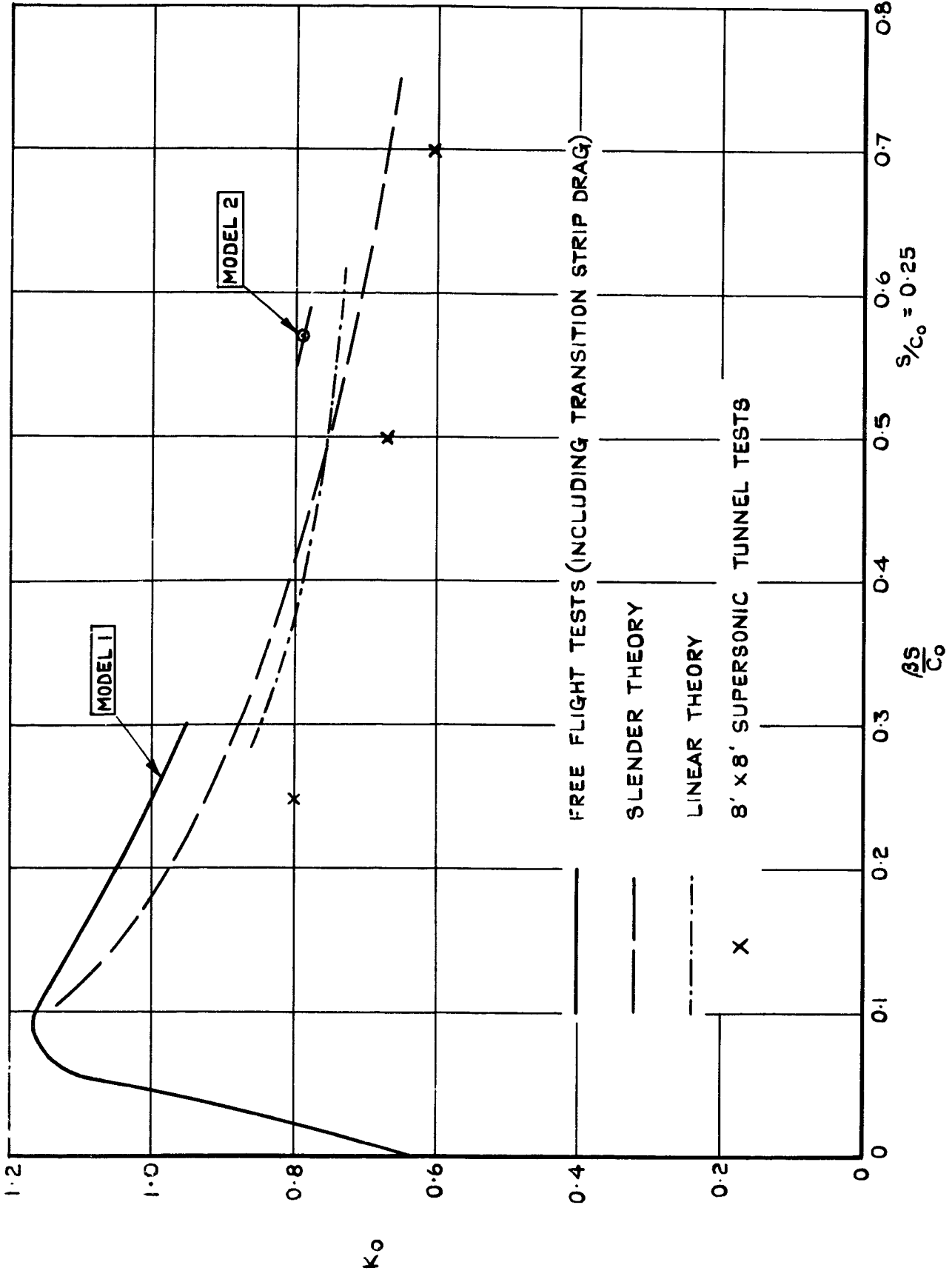


FIG. 6. ZERO-LIFT WING WAVE DRAG FACTOR K_0 .

A.R.C. C.P. No. 670

533.693.3:
533.6.013.12:
533.6.011.35/5

FREE-FLIGHT MEASUREMENTS OF THE ZERO-LIFT DRAG OF A
SLENDER OGEE WING AT TRANSONIC AND SUPERSONIC SPEEDS. Edwards, J.B.W.
Oct. 1962.

The zero-lift drag of a slender-wing model has been measured using the free-flight technique and the wing wave drag has been deduced by subtracting the non-wave-drag components.

The results are presented without correction for the drag increment caused by the transition strip and show a smooth variation of the wave drag factor K_0 with Mach number with a maximum occurring near $M = 1.1$. The overall level of K_0 is some 10% higher than that predicted by linear theory, but this result is very dependent on the accuracy of the skin-friction estimates as well as on the transition strip drag increment. Attempts to estimate the latter suggest that 4% of the total drag may arise from this source which would reduce K_0 by some 12% bringing it well in line with theory.

A.R.C. C.P. No. 670

533.693.3:
533.6.013.12:
533.6.011.35/5

FREE-FLIGHT MEASUREMENTS OF THE ZERO-LIFT DRAG OF A
SLENDER OGEE WING AT TRANSONIC AND SUPERSONIC SPEEDS. Edwards, J.B.W.
Oct. 1962.

The zero-lift drag of a slender-wing model has been measured using the free-flight technique and the wing wave drag has been deduced by subtracting the non-wave-drag components.

The results are presented without correction for the drag increment caused by the transition strip and show a smooth variation of the wave drag factor K_0 with Mach number with a maximum occurring near $M = 1.1$. The overall level of K_0 is some 10% higher than that predicted by linear theory, but this result is very dependent on the accuracy of the skin-friction estimates as well as on the transition strip drag increment. Attempts to estimate the latter suggest that 4% of the total drag may arise from this source which would reduce K_0 by some 12% bringing it well in line with theory.

A.R.C. C.P. No. 670

533.693.3:
533.6.013.12:
533.6.011.35/5

FREE-FLIGHT MEASUREMENTS OF THE ZERO-LIFT DRAG OF A
SLENDER OGEE WING AT TRANSONIC AND SUPERSONIC SPEEDS. Edwards, J.B.W.
Oct. 1962.

The zero-lift drag of a slender-wing model has been measured using the free-flight technique and the wing wave drag has been deduced by subtracting the non-wave-drag components.

The results are presented without correction for the drag increment caused by the transition strip and show a smooth variation of the wave drag factor K_0 with Mach number with a maximum occurring near $M = 1.1$. The overall level of K_0 is some 10% higher than that predicted by linear theory, but this result is very dependent on the accuracy of the skin-friction estimates as well as on the transition strip drag increment. Attempts to estimate the latter suggest that 4% of the total drag may arise from this source which would reduce K_0 by some 12% bringing it well in line with theory.

© *Crown copyright* 1964

Printed and published by

HER MAJESTY'S STATIONERY OFFICE

To be purchased from

York House, Kingsway, London W.C.2

423 Oxford Street, London W.1

13A Castle Street, Edinburgh 2

109 St. Mary Street, Cardiff

39 King Street, Manchester 2

50 Fairfax Street, Bristol 1

35 Smallbrook, Ringway, Birmingham 5

80 Chichester Street, Belfast 1

or through any bookseller

Printed in England